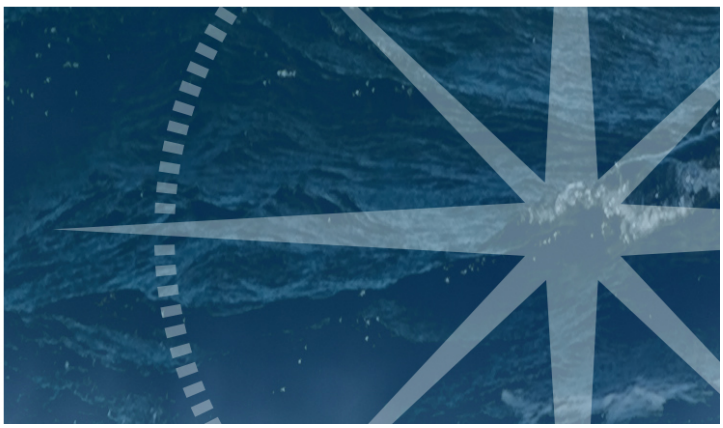

MONALISA 2.0 – Activity 4

Report on case study on Manoeuvring/Recovering of damaged ships

Document No: MONALISA 2 0_D 4.2.2

Co-financed by the European Union
Trans-European Transport Network (TEN-T)

Document name	Report on task T.4.2.2
Title	Report on case study on Manoeuvring/Recovering of damaged ships
Activity	4
Subject	Operational Safety
Sub-activity	4.2
Subject	Safety in Coastal Areas
Sub. Act. Leader	SASEMAR
Deliverable Developer	Compass IS, S.A.

INDEX OF CONTENTS

INDEX OF CONTENTS 3

1. Introduction 5

2. Scenario for live exercise 6

3. Scenario for computer simulations 8

3.1. Procedence and data gathering 9

3.2. Waves data 9

3.3. Wind data 10

3.4. Currents data 11

3.5. Case study: Sea state 12

4. Passenger ship for the case study/simulations 13

"Fortuny" main particulars 13

3D CAD model 13

5. Tugboat for the case study/simulations 14

"Sar Mesana" main particulars 14

Hull shape drawing 14

3D CAD model 15

6. Computational analysis performed for the case study 16

6.1. Main goal of the simulations 16

6.2. Definition and creation of the 3D CAE models for the simulations 16

- Ship condition 16

6.3. Ships´ hydrostatic data 18

- Data for *Sar Mesana* 18
- Data for *Fortuny* 19

6.4. Towing configuration 20

6.5. Environment conditions 23

6.6. Numerical data for the simulation 24

7. Resuts from the case study simulation 25

7.1. Body dynamics of both ships 25

7.2. Tension on the towing line 28

7.3. Visual output of the simulation 29

8. Conclusions 35
9. Annex I: Seakeeping/Manoeuvring code for simulations: SeaFEM 37
10. Annex: Cable model in SeaFEM for towing simulations 38
10.1. Introduction 38
10.2. Formulation 38
10.3. Forces acting on the line 40
10.4. Temporay integration scheme 40
10.5. Coupling with SeaFEM 41

1. Introduction

The work during this period has been focused on the definition and simulation of a case study on manoeuvring/recovering of damaged ships, after the definition of the scenario for Maritime Search and Rescue exercise, this latter task having been performed by SASEMAR

For defining the case study and the simulations, the data previously gathered, regarding scenario´s sea and weather conditions and involved ships´ characteristics, and has been used. Other data –like tugboat´s operation- which was not so clear for Compass staff, has been detailed by qualified personnel from SASEMAR. The data used for the simulations corresponding to this case study can be summarized in the following points:

- Sea zone where the exercise will take place. This will set the simulations domain depth parameter and determine the sea conditions.
- Sea conditions: waves´ height and period, wind, and currents.
- Passenger ship´s characteristics and hull geometry.
- Tugboat´s characteristics and hull geometry.
- Initial load and hydrostatic condition of the passenger ship (heeling, sinking and trim).
- Tugboat operation during the exercise. This will also define some parameters for the simulations.

2. Scenario for live exercise

The scenario is set by SASEMAR. The details are explained in the following lines, and reproduces what is explained in previously produced document, submitted by SASEMAR. The following picture, provided by SASEMAR, shows the **scenario**:

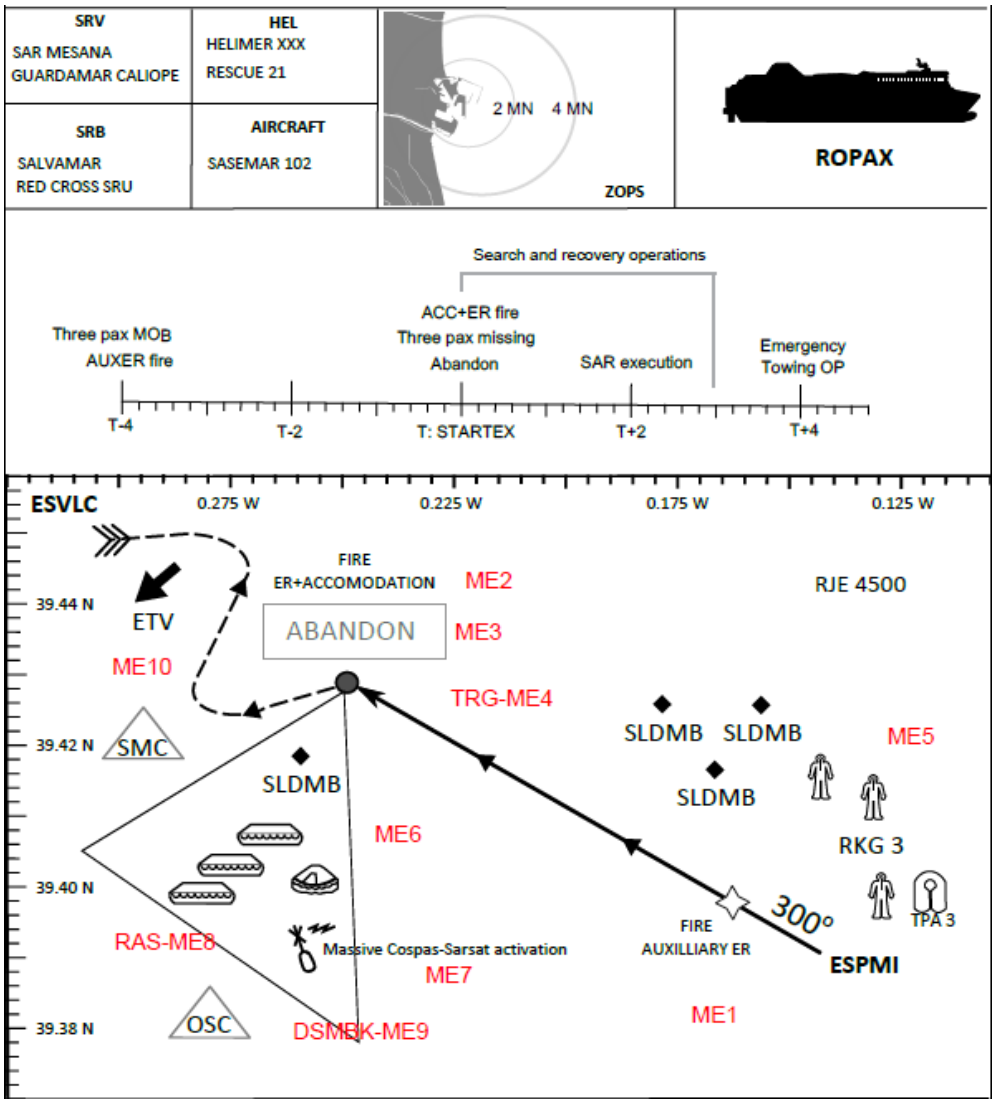

Figure 1: SAREX Monalisa MRO Live Exercise

Scenario narrative:

1. A fire breaks out in the auxiliary engine room on board of the passenger vessel. The ship has sailed from Palma de Mallorca to Valencia after completing her last port call. The fire is located in the way of the auxiliary engine´s fuel supply module, and quickly spreads across the compartment.
2. After two hours fighting the fire, the crew is able to extinguish it, and the vessel is underway using the main engine.
3. Few hours later, a second fire breaks out on the deck above the auxiliary engine room and smoke spreads to adjacent compartments, including the engine room control room and remote passenger accommodation areas.
4. Fixed local application (water mist) and bilge (low expansion foam) fire extinguishing systems are activated, but do not completely extinguish the fire. The Captain issues the order to abandon ship.
5. After a role call, three passengers are declared missing.
6. Fire occurred when the pressure regulation valve´s actuator diaphragm ruptured, and fuel oil sprayed on exposed high temperature surface on an adjacent auxiliary engine.
7. The fire causes the ship to lose electrical power which finally requires her to be towed to Valencia for repairs.

Regarding the simulations performed for the case study, only the last point of this scenario is relevant. Furthermore, the simulations correspond to the *transport* phase, where the damaged ship is being towed already at a constant speed, not the actual rescue phase.

3. Scenario for computer simulations

Concerning the definition of the case study, and in order to be able to perform useful numerical simulations, some information regarding sea conditions near the exercise scenario has been gathered.

In following sections of this document, it is explained how this information is used inside the seakeeping computer simulation code (SeaFEM).

The information has been obtained from the web site of *Puertos del Estado* (*Ministerio de Fomento, Gobierno de España*):

http://www.puertos.es/en/oceanografia_y_meteorologia/redes_de_medida/index.html

Figure 2: Situation of the data buoys near the exercise location

Two data buoys in the surroundings of the exercise localization have been chosen for gathering the needed information. One buoy for waves and winds:

WANA-2081113 Node

- Longitude: **-0.25 E**
- Latitude: **39.417 N**
- Depth: **undefined**

And another buoy for the currents (already dismantled, but the only one with currents data in the zone):

Valencia I buoy

- Longitude: **0.25 W**
- Latitude: **39.46 N**
- Depth: **28 m**

3.1.Procedence and data gathering

The WANA data consists of temporal series of wind, currents and waves parameters coming from numerical models. WANA series are derived from the prediction system that *Puertos del Estado* has developed together with the *Agencia Estatal de Meteorología* (*AEMET*).

The relevant data is summarized in the following charts. With this data, sea states will be generated for the simulations.

3.2.Waves data

For generating the waves´fields a WAM model is used. Such model is an spectral model which solves the energy ballance equation. It works in the Mediterranean sea with a resolution of 0.125 degrees (15 km).

Waves´ peak period and significant height (annual, January 1996-October 2013):

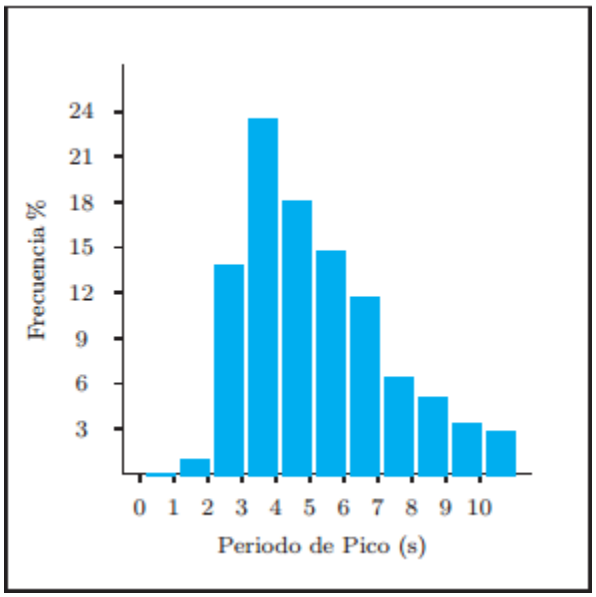

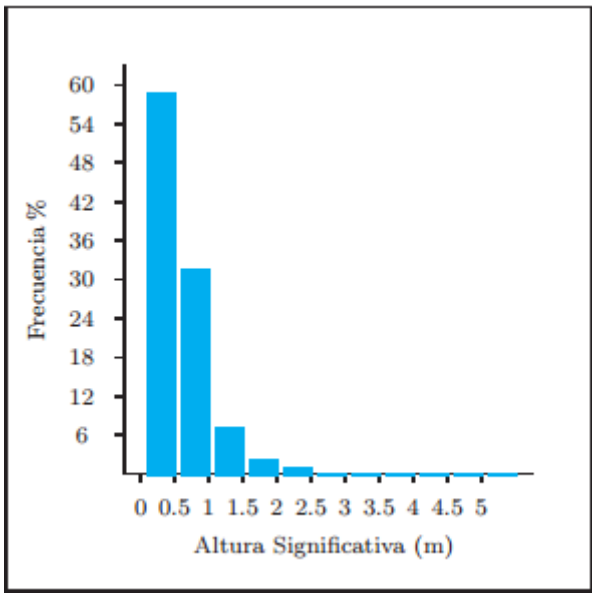

Waves´ directions and significant height (annual, January 1996-October 2013):

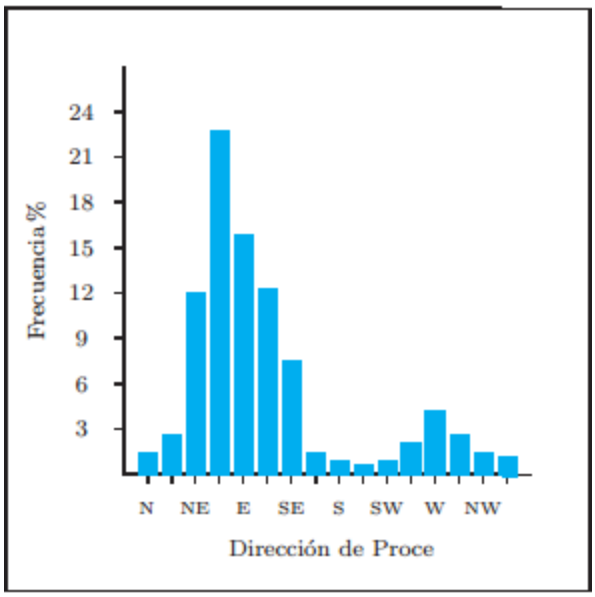

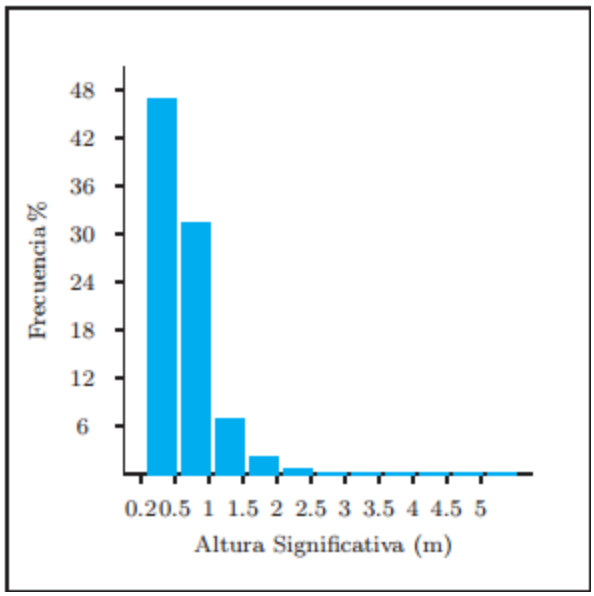

3.3.Wind data

The atmospheric model used for generating the wind fields is HIRLAM. It is a mesoescalar and hydrostatic model with a resolution of 0.2 degrees in the Mediterranean sea. The wind data obtained are hour-averaged, at 10 metres above sea level.

Wind directions and average velocity (annual, January 1996-October 2013):

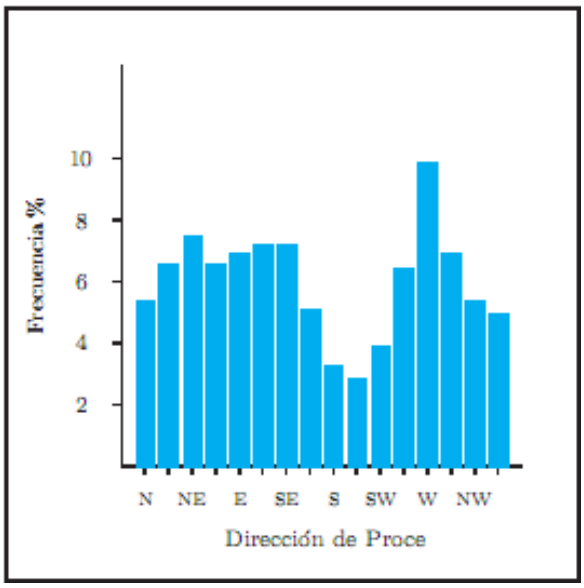

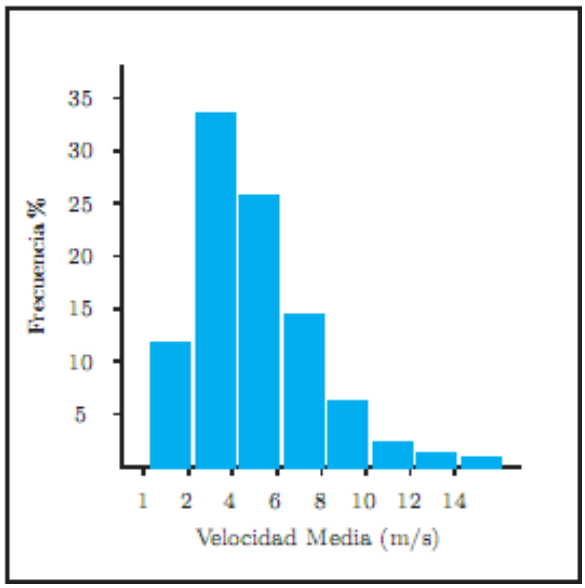

Wind directions (annual, January 1996-October 2013):

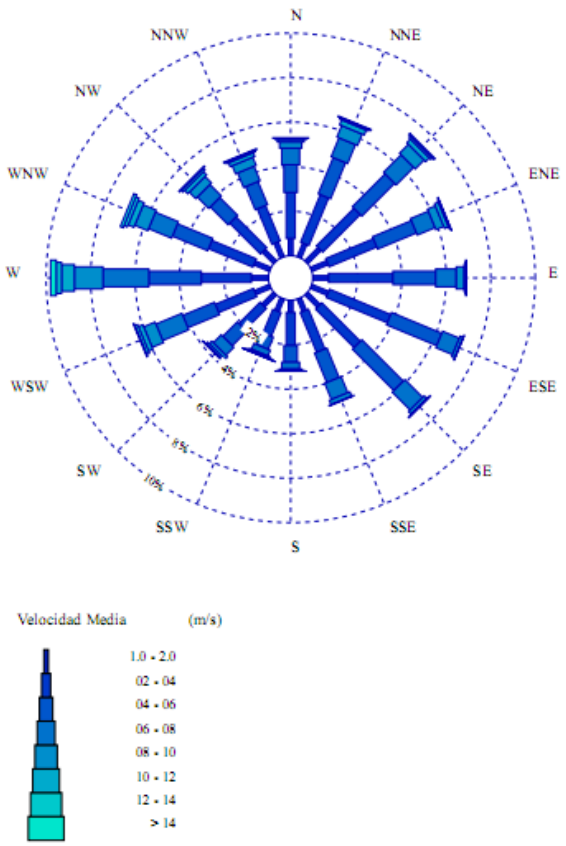

3.4.Currents data

Currents velocity and direction:

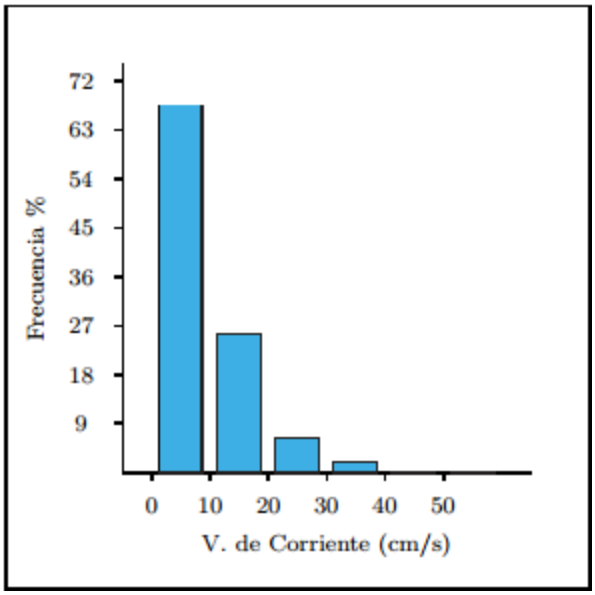

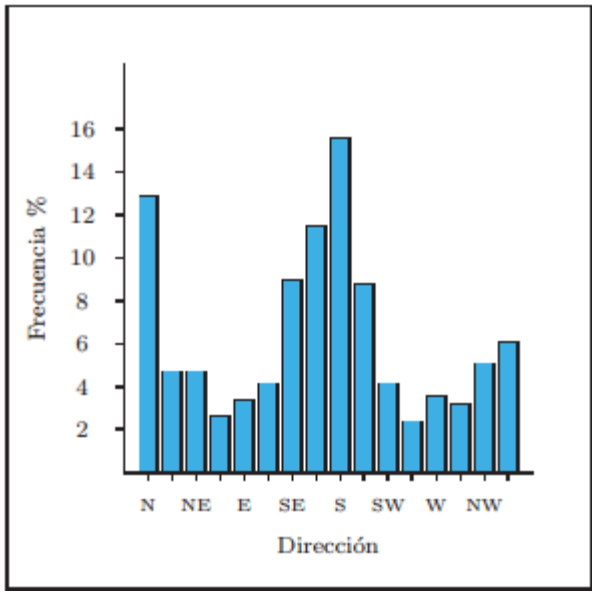

3.5.Case study: Sea state

Based in average figures taken from previous data, a sea condition has been figured out, in order to reproduce it in the simulations. For waves, **Pearson-Moskowitz** spectrum will be used, therefore the wave data showed corresponds to the parameters needed for using such wave spectrum model. For the actual case study simulation, the following data has been used:

Case study: Sea state

Wind direction (deg)	270 (W)
Wind average speed (m/s)	4
Hs (m)	3.0
T (average) (s)	5
T (max) (s)	12
T (min) (s)	3
Direction (deg)	112.5 (ENE)
Spread. Angle (deg)	45

4. Passenger ship for the case study/simulations

The passenger ship chosen for performing the simulations is the **"Fortuny"** (or its twin ***"Sorolla"***). General arrangement drawings of the ship are available, and have been provided by SASEMAR. Compass IS has generated a three-dimension CAD model of the vessel in order to generate the case study and perform simulation tests.

Hydrostatic, centre of gravity and stability will be estimated from general data of similar passenger ships.

"Fortuny" main particulars

- Length overall: **172 m**
- Length between perpendiculars: **157 m**
- Moulded breadth: **26.2 m**
- Depth: **14.84 m**
- Average draught (at max. load): **6.20 m**
- Displacement (at max. load): **16555 T**

3D CAD model

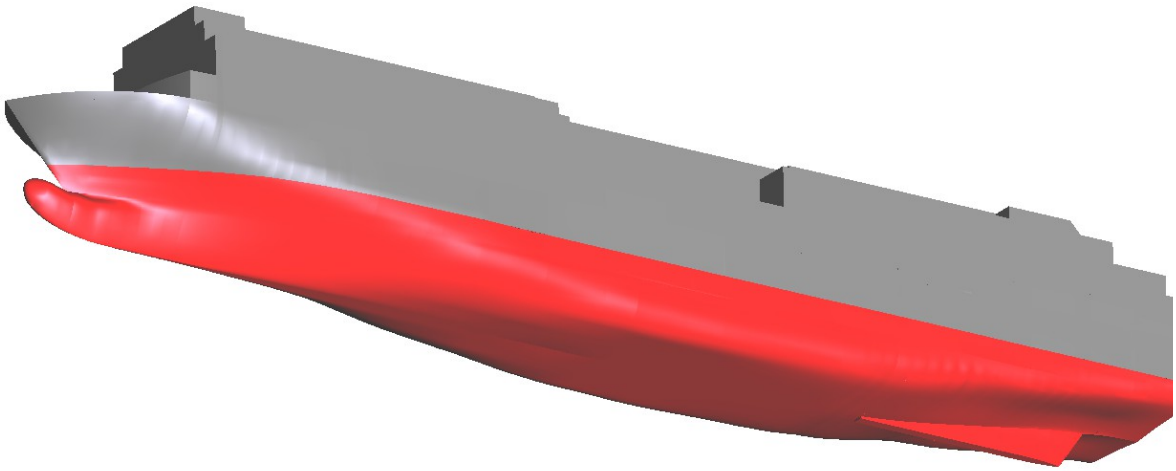

Figure 3: ROPAX "Fortuny", 3D CAD model

5. Tugboat for the case study/simulations

SASEMAR has provided hull shape drawings, hydrostatic and stability data of three different tugboats, but finally the ship chosen for the simulations will be **"Sar Mastelero"** (same ship construction series as **"Sar Mesana"**)

"Sar Mesana" main particulars

- Length overall: **39.699 m**
- Length at water line: **37.576 m**
- Length between perpendiculars: **34.520 m**
- Moulded breadth: **12.5 m**
- Depth: **5.8 m**
- Project draught: **4.2 m**
- Displacement (at project draught): 1124 T

Hull shape drawing

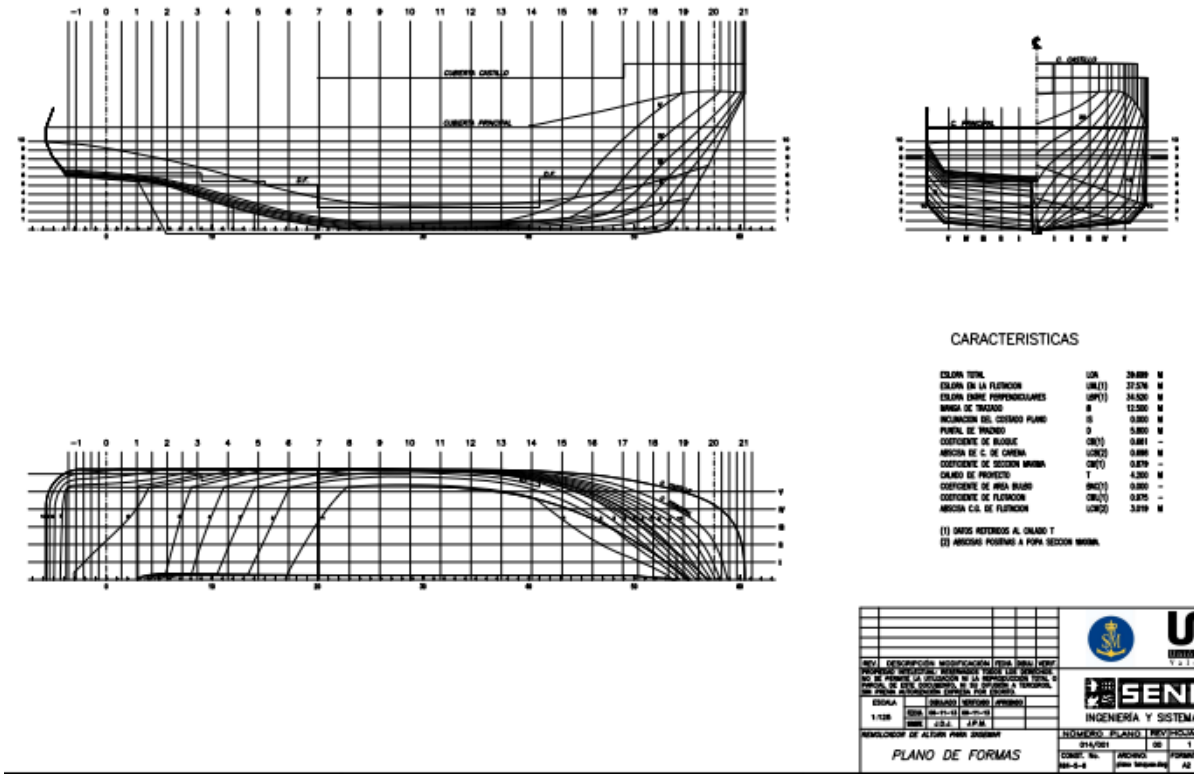

Figure 4: Tugboat "Sar Mesana", Hull shape drawing

3D CAD model

From the previous drawing, a three-dimensional CAD model has been generated, in order to include the ship in the simulations:

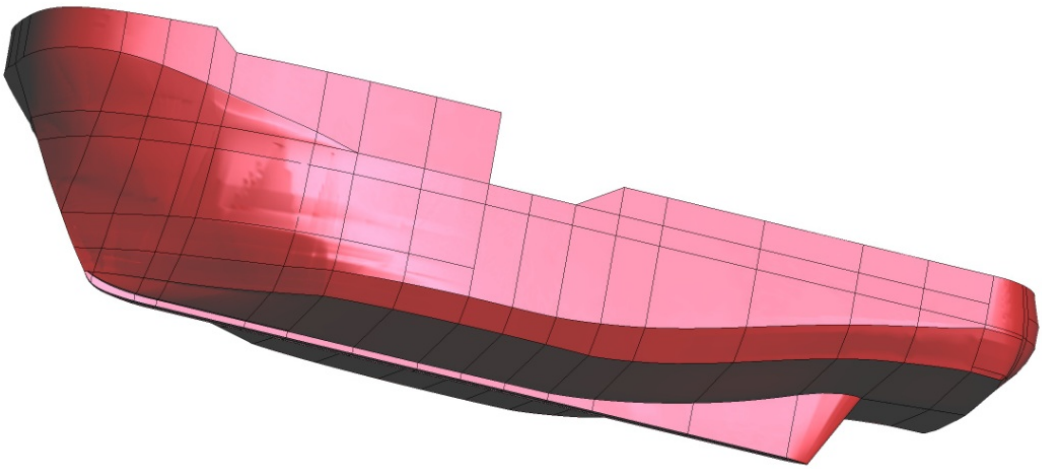

Figure 5: Tugboat “Sar Mesana”, 3D CAD model

6. Computational analysis performed for the case study

The computer simulations will be carried out by means of the **seakeeping solver SeaFEM**, which is a suite of tools for computational analysis of the effect of waves, wind and currents on naval and offshore structures.

Furthermore, SeaFEM is an state-of-art radiation and diffraction potential solver which performs direct time-domain analyses of the dynamic response of the structure. More details of SeaFEM can be found in Annex I.

6.1. Main goal of the simulations

The main goals of the study are:

- Identifying the feasibility of the towing operation under different sea and wind conditions. For this purpose, the simulations will provide the history of movements and forces acting on the different ships. A statistical analysis of that history (average value, maximum and standard deviation) can also be obtained.
- Obtaining forces acting on the towing lines. Furthermore, the forces acting on the towing lines can be thoroughly analysed. The tension evolution in the lines during the different cases to be studied will be evaluated. Again, a statistical analysis of the tension history (average value, maximum and standard deviation) will be performed.
- Giving assessment regarding the possible risk of failure of the towing line in different conditions.

6.2. Definition and creation of the 3D CAE models for the simulations

For the case study simulation of a *transport* **towing condition,** an initial situation for the passenger vessel has been considered:

- **Ship condition**

  Upright condition.

  Loading condition:

  - Displacement: **18577.3 T** (10-11% of displacement at max. load)
  - Draught: **6.8 m** (corresponding to above displacement)

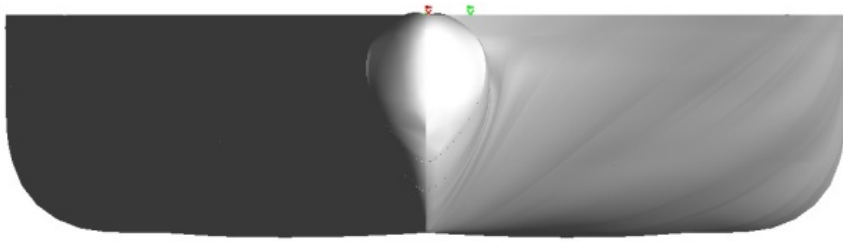

Figure 6: ROPAX "Fortuny", upright condition

This ship´s condition will be combined with the sea state previously defined (configured from the waves, and wind data gathered, as mentioned in section 3).

A computational domain including the ships´ hull geometry needs to be arranged in SeaFEM. The corresponding *Fortuny* and *Sar Mesana* 3D CAD hull geometries are directly imported to the Graphic User Interface. The following image shows the computational domain:

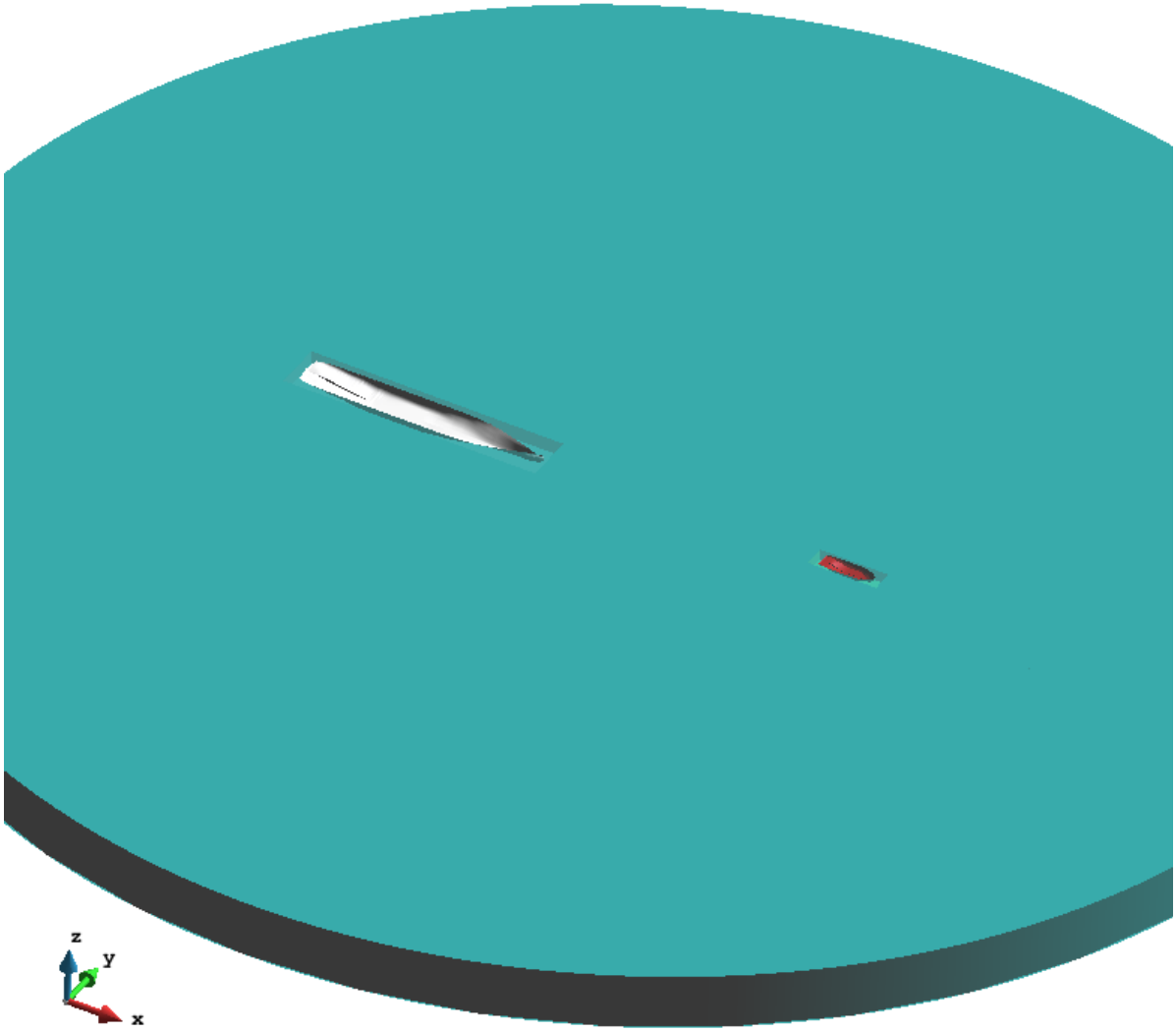

Figure 7: Computational domain including both ships

6.3. Ships´ hydrostatic data

The data corresponding to both hulls, at the defined loading condition needs to be inserted in SeaFEM, in order to perform the simulations. This data includes displacement for the given condition, center of gravity position, radii of gyration and external forces.

- **Data for *Sar Mesana***

In this case, the surge and yaw degrees of freedom are restrained.

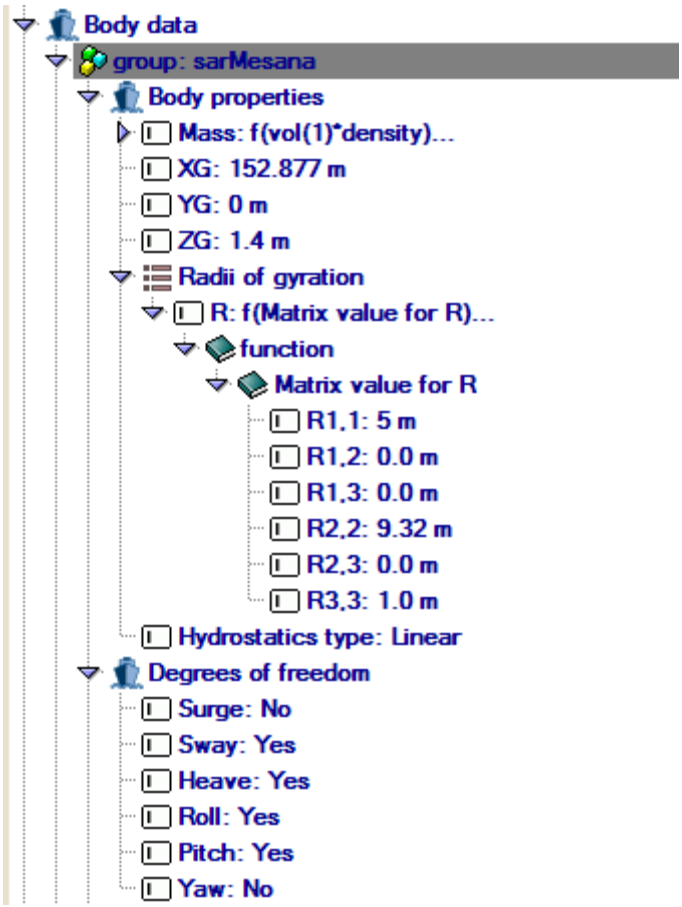

- **Data for *Fortuny***

For this ship, all degrees are considered unrestrained. Also, **external forces** corresponding to **wind** and **drift** forces are included.

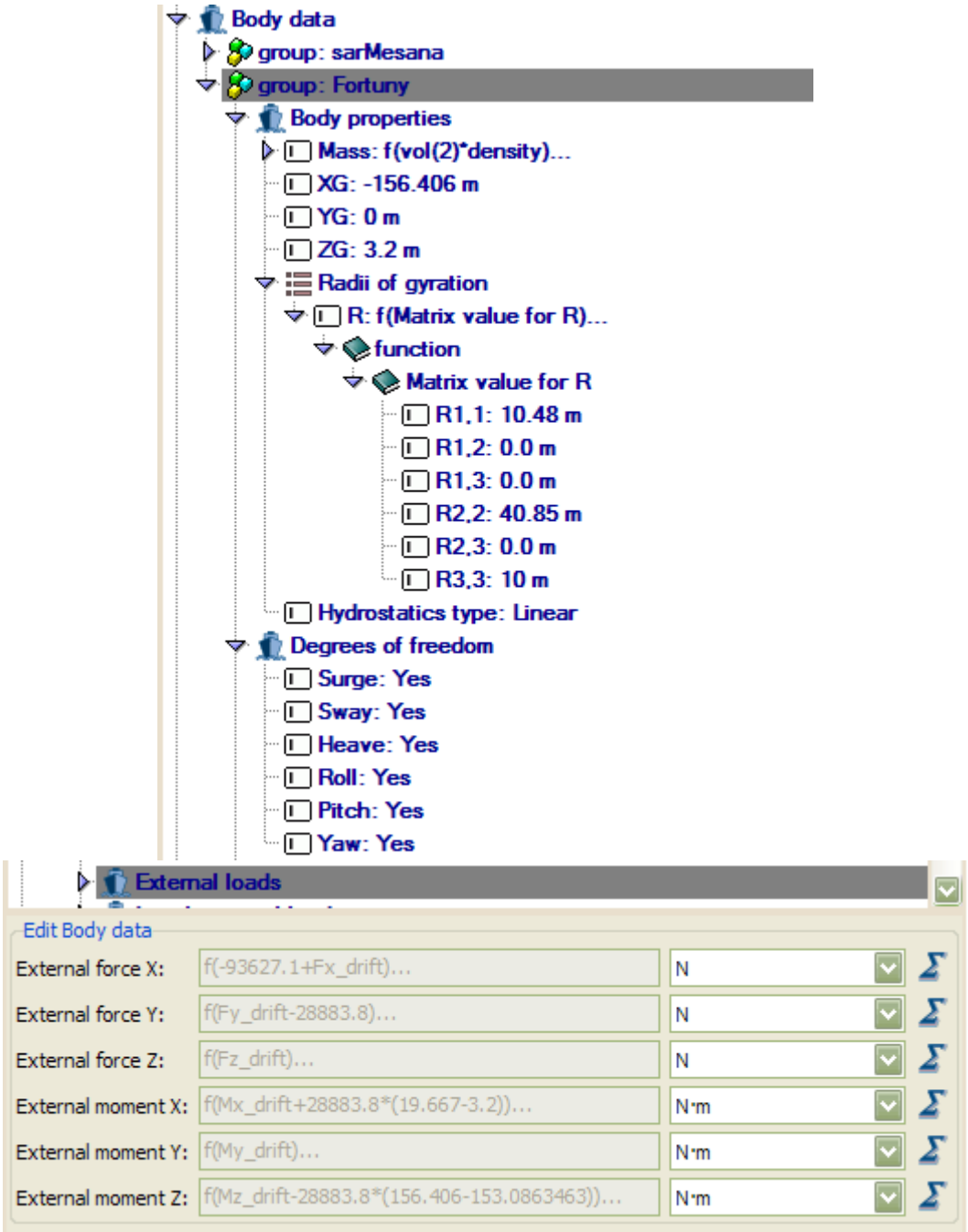

6.4.Towing configuration

Regarding the towing configuration itself, details of how such operation is performed have been provided by SASEMAR. For the case study, a **transport towing** at a **constant sustained speed of 8 knots** has been considered.

With this information, which also includes the towing lines´ materials, it is possible to define the simulation for the case study.

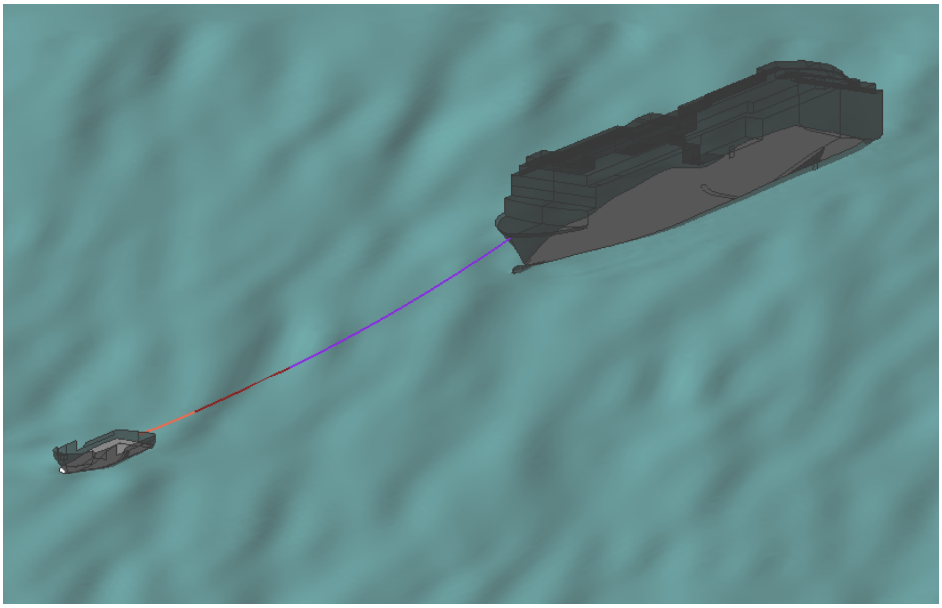

Figure 8: Initial configuration of the towing operation

Materials´properties for the towing line are also inserted in the graphic user interface. These properties have been provided by SASEMAR qualified staff, as mentioned before.

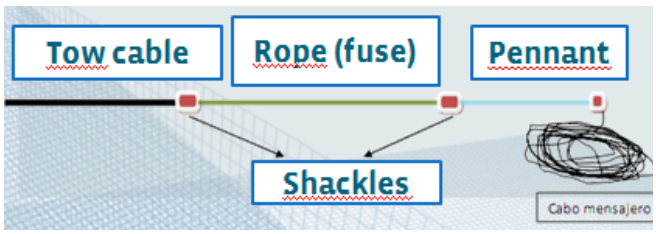

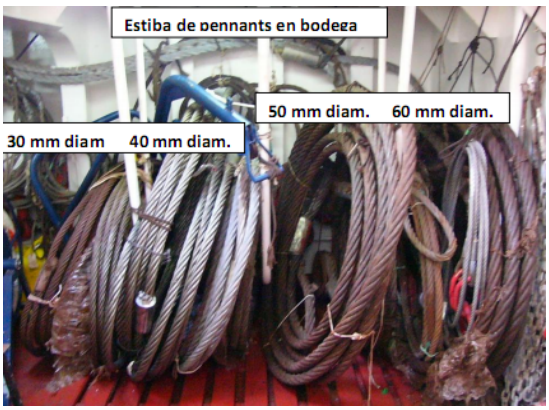

	Tug cable	Rope	Pennant
Length (m)	**120.5**	**50**	**30**
Area (m2)	**0.00181**	**0.00502**	**0.00282**
Young Modulus (Pa)	**2.1e11**	**3.0e9**	**2.1e11**
Effective weight (N/m)	**139.15**	**61.08**	**217.43**
Material	**Steel**	**Nylon**	**Steel**

6.5. Environment conditions

SeaFEM allows defining different **sea waves spectrums**, and **currents**. Also external forces can be defined to model **wind forces**, as shown in previous sections. In this case, **Pierson-Moskowitz** spectrum will be used, with the sea conditions data described in section 3 of this document. Also, location depth is inserted in SeaFEM graphic user interface:

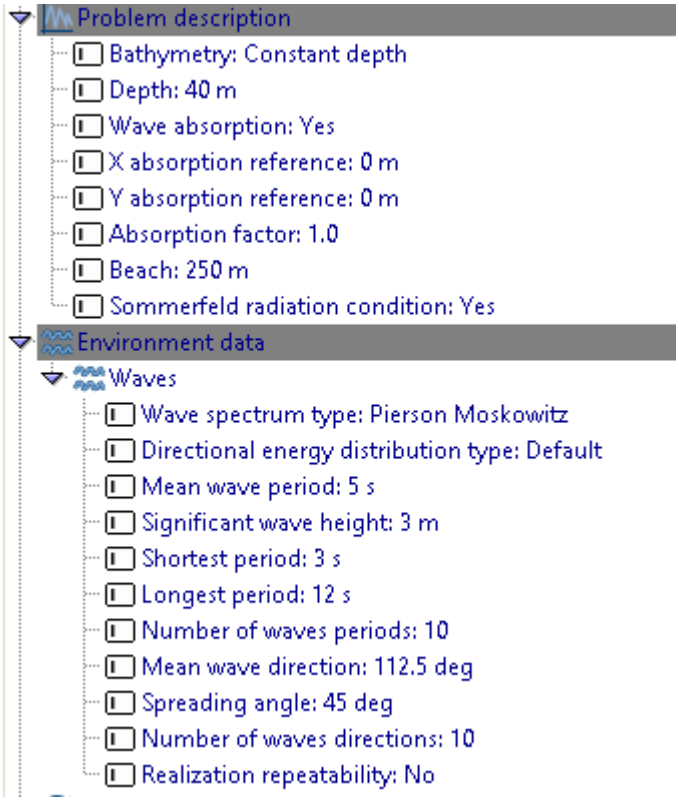

Figure 9: Environment conditions

6.6. Numerical data for the simulation

The analysis was carried out with the following numerical and solver parameters:

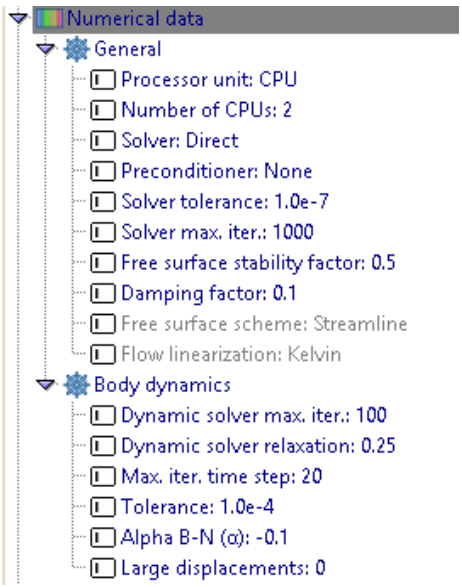

Figure 10: Numerical parameters

Regarding time step, it must be noted that it is autommatically calculated in order to fulfill free surface stability factor criteria, together with mesh volume elements size below the free surface. In this case, the **time step** was **dt = 0.06427 seconds**. **Total physical simulated time** was **300 seconds.**

7. Resuts from the case study simulation

Different useful results can be retrieved from the seakeeping simulations performed with SeaFEM. The most relevant for this case study, are:

- Time history of motions of both damaged ship and tug boat (body dynamics).
- Time history of force acting on the tow line.
- Free surface elevation evolution during the simulation: incident waves (waves' spectrum) and radiated and diffracted waves due to interaction with the moving bodies.

7.1. Body dynamics of both ships

The following graphs show the most relevant body dynamics of tug boat (*Sar Mesana*):

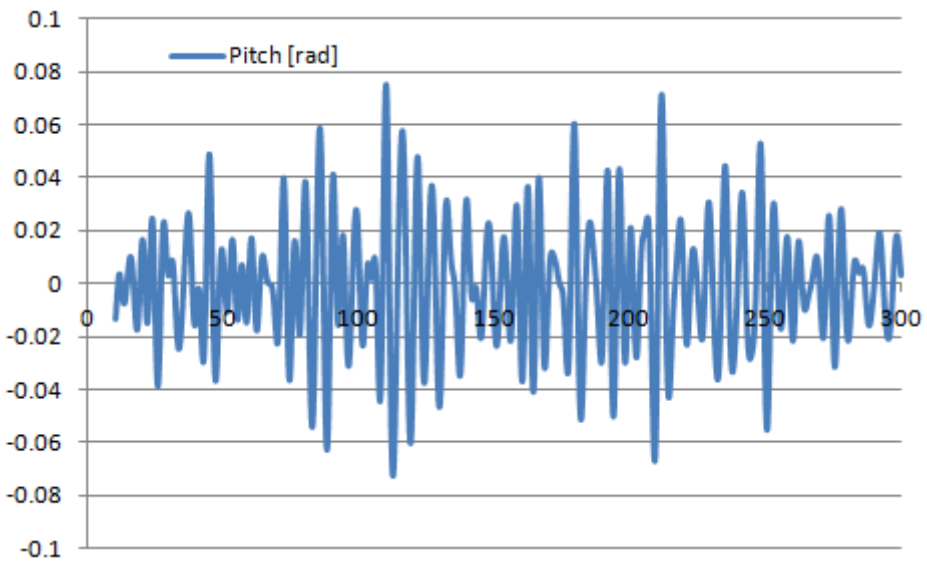

Figure 11: Pitch time history for Sar Mesana

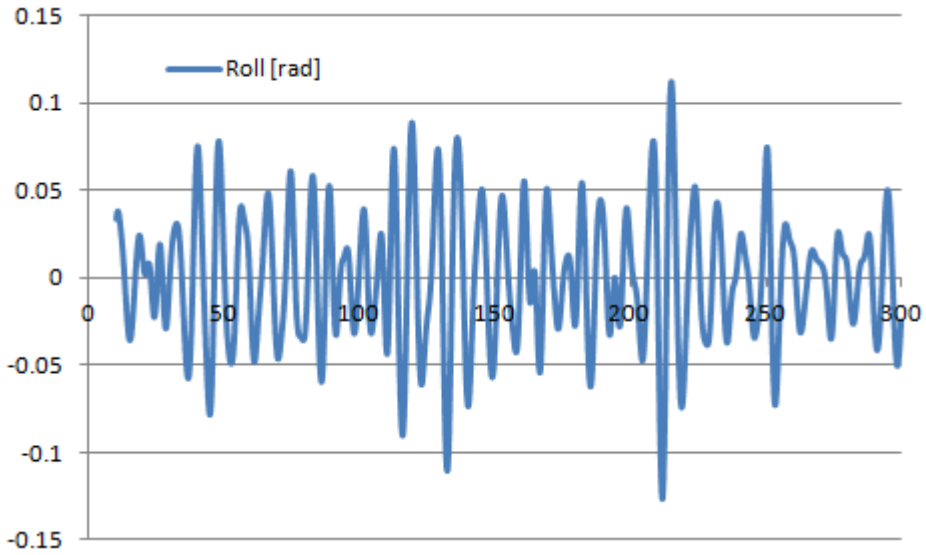

Figure 12: Roll time history for Sar Mesana

The next graphs show the most relevant body dynamics of damaged ship (*Fortuny*):

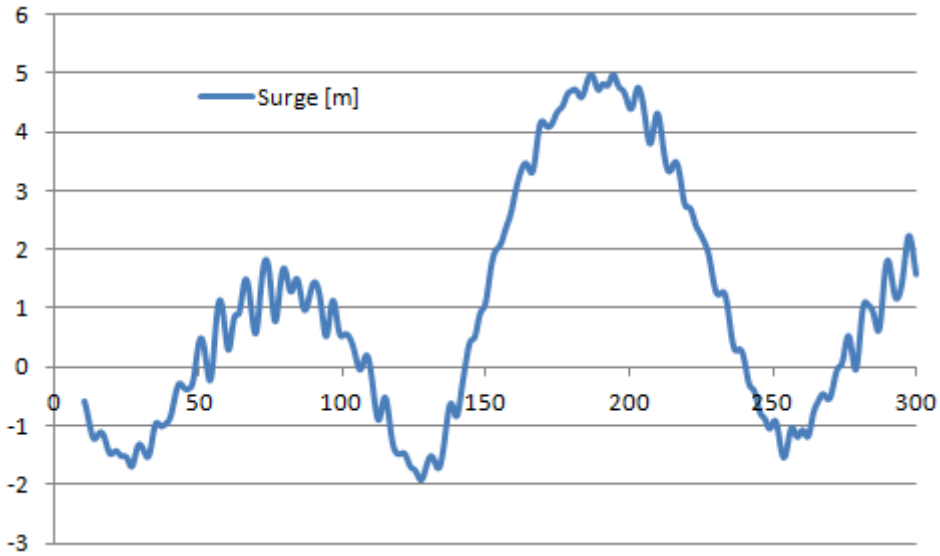

Figure 13: Surge time history for Fortuny

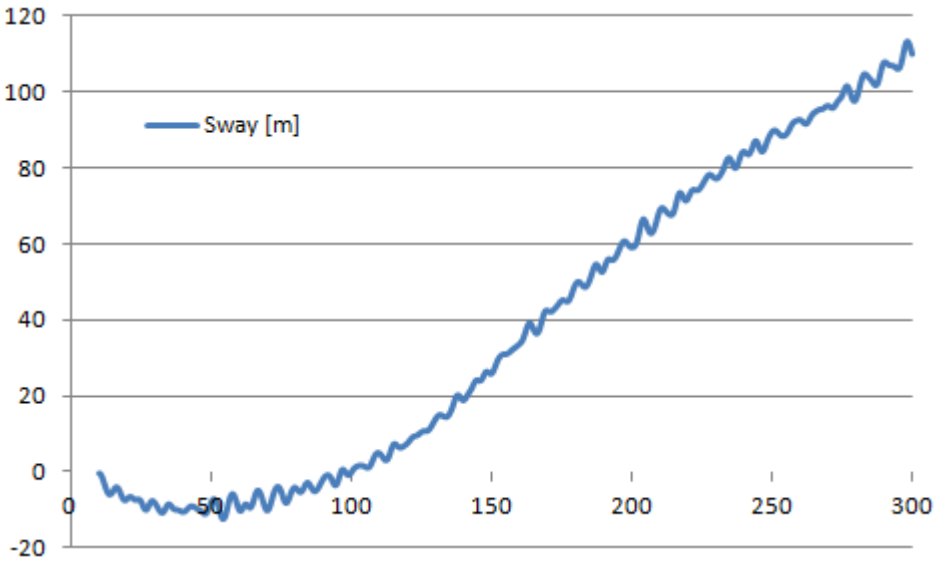

Figure 14: Sway time history for Fortuny

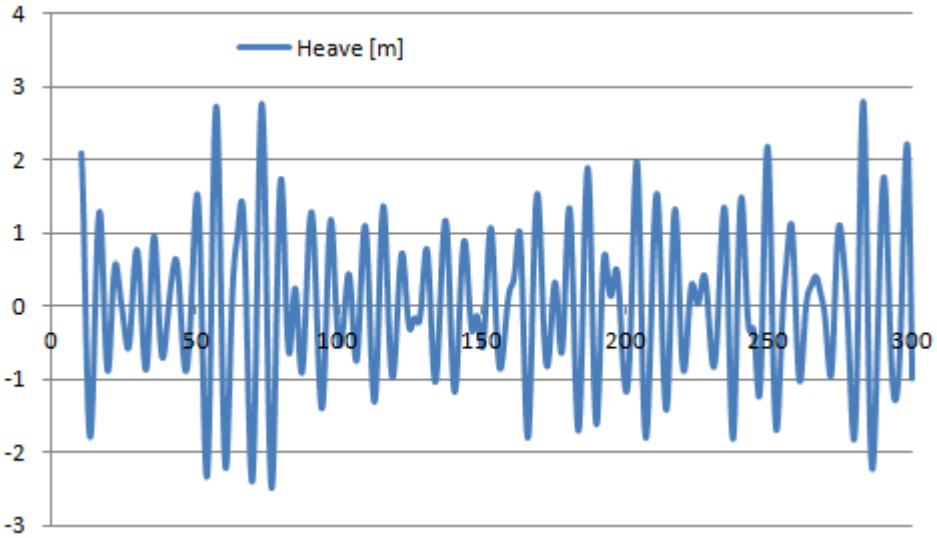

Figure 15: Heave time history for Fortuny

7.2. Tension on the towing line

The following graphs show the longitudinal (X axis) and vertical (Z axis) components of the force acting on the towing line:

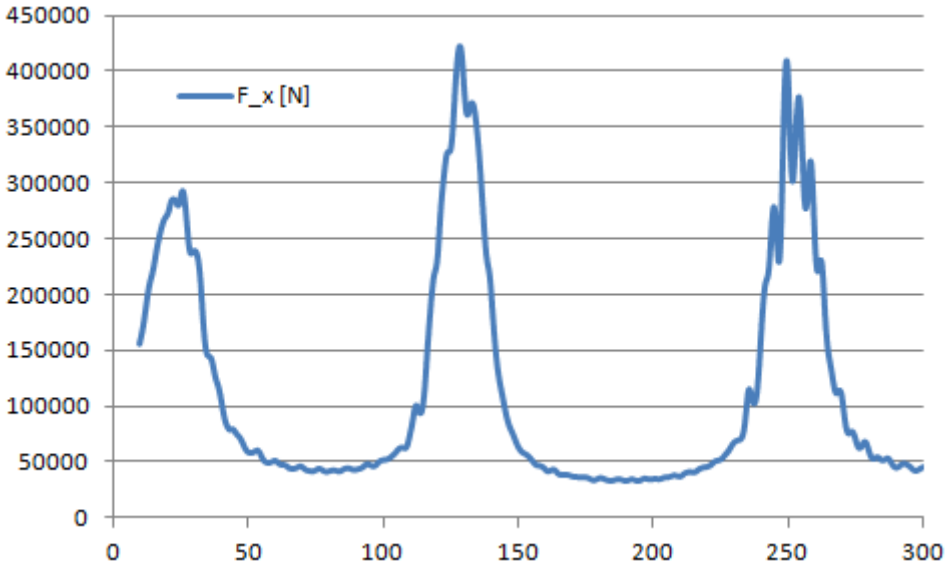

Figure 16: Horizontal force's evoution on the towing line

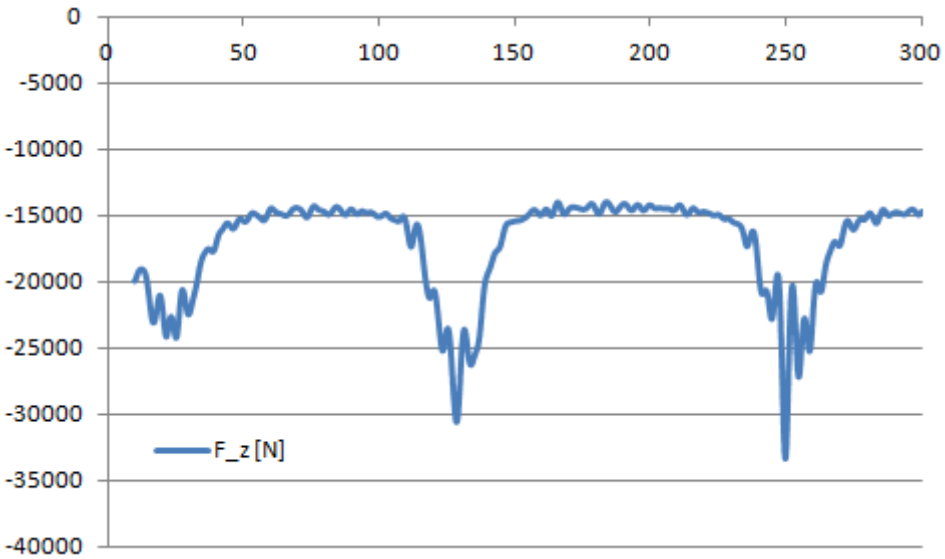

Figure 17: Vertical force's evolution on the towing line

7.3. Visual output of the simulation

The next images show the position evolution of the ships at different stages of the simulation, due to the wind, waves and drift forces, from initial time step (t = 10 s), to final time step (t = 300 s):

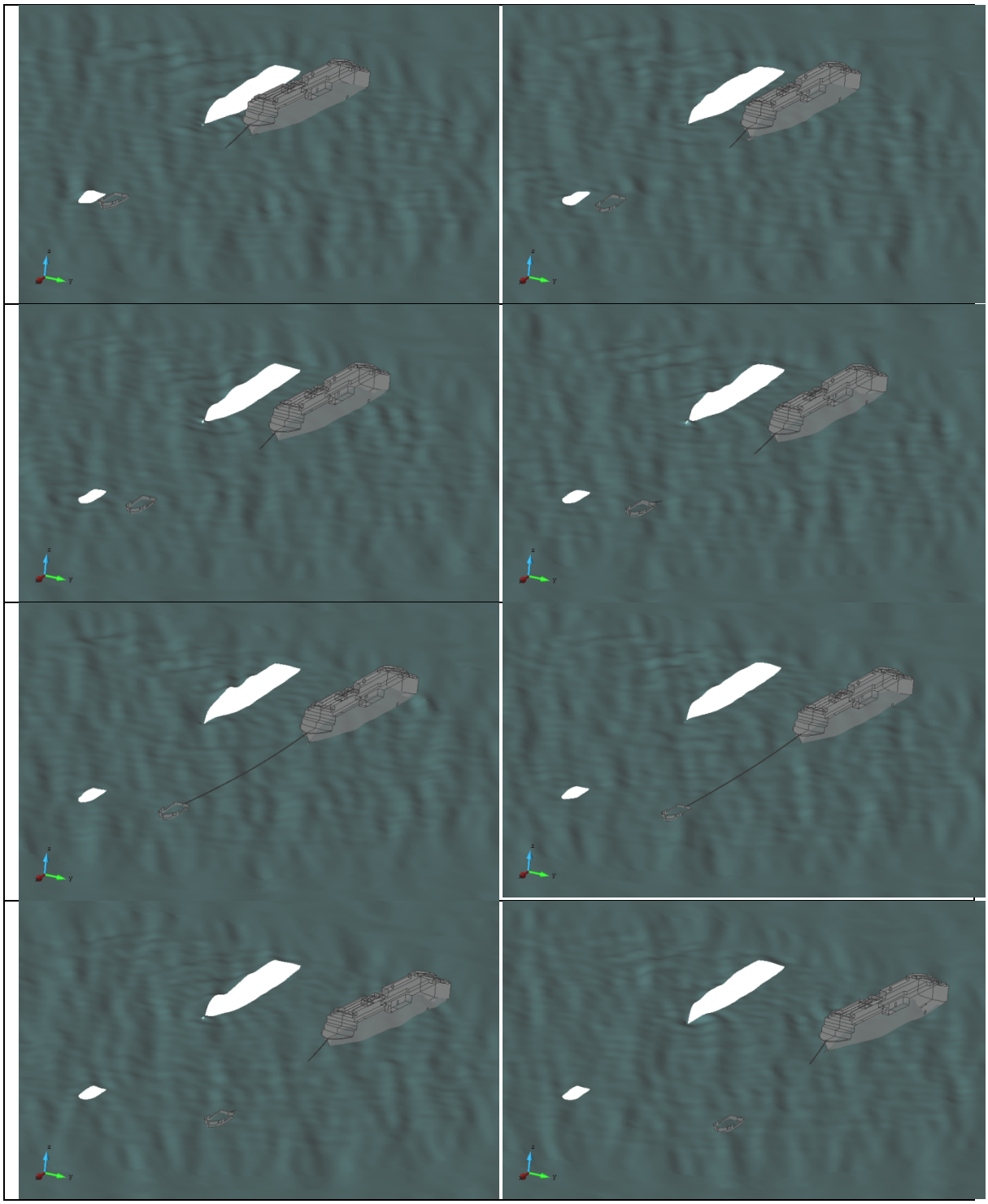

The following images show a lateral view of different steps of the simulation results:

Figure 18: Lateral view, t=10 s

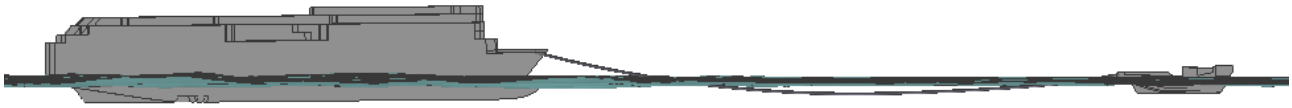

Figure 19: Lateral view, t=50 s

Figure 20: Lateral view, t=100 s

Figure 21: Lateral view, t=120 s

Figure 22: Lateral view, t=200 s

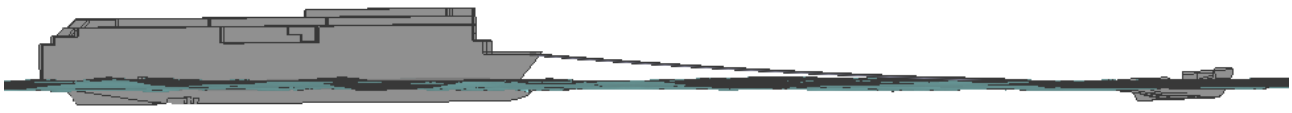

Figure 23: Lateral view, t=250 s

The following images show a zenital view of different steps of the simulation results:

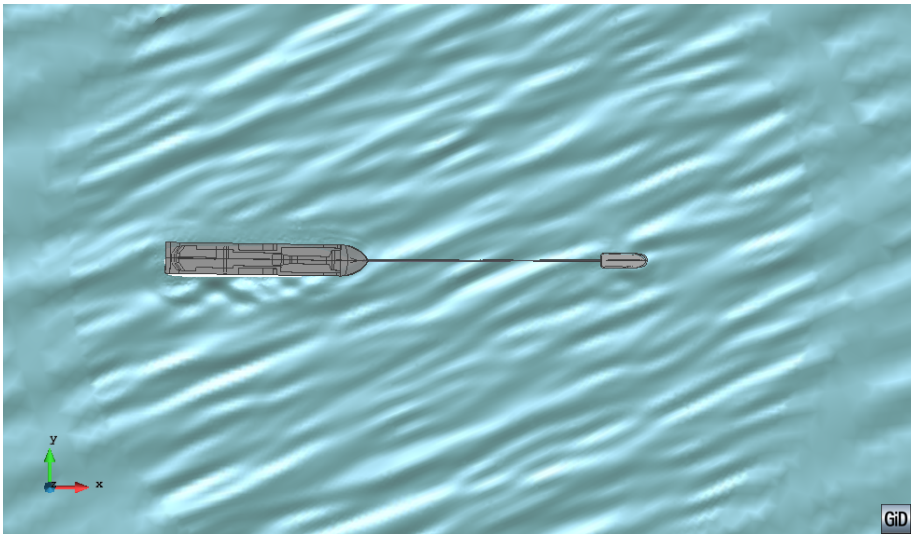

Figure 24: Zenital view, t=10 s

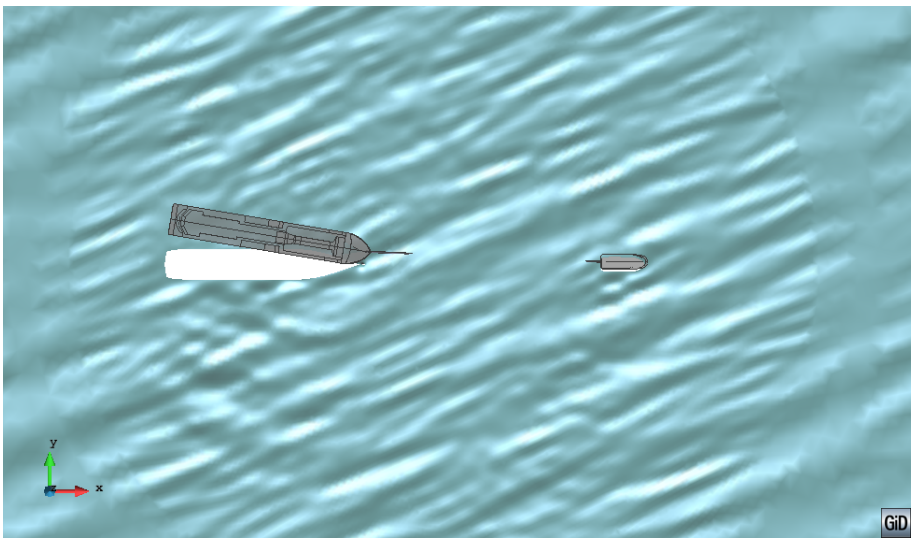

Figure 25: : Zenital view, t=100 s

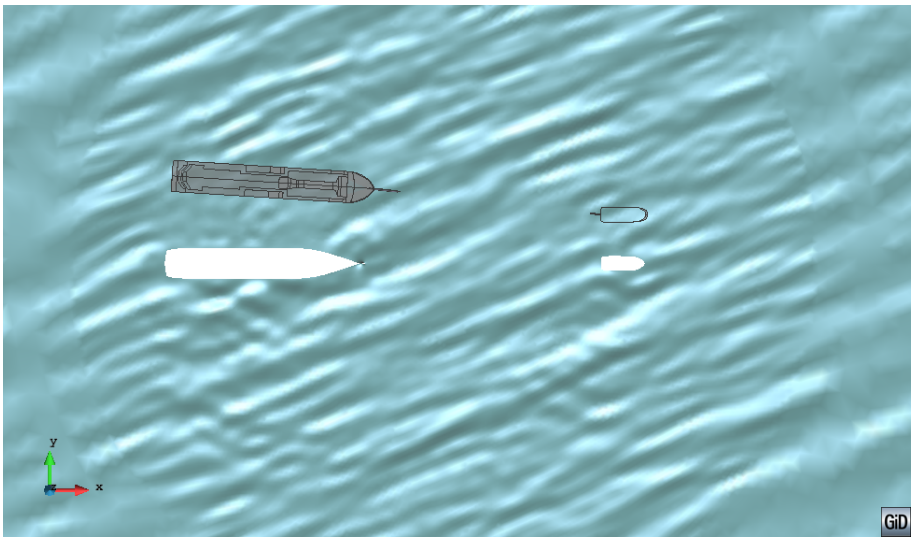

Figure 26: : Zenital view, t=200 s

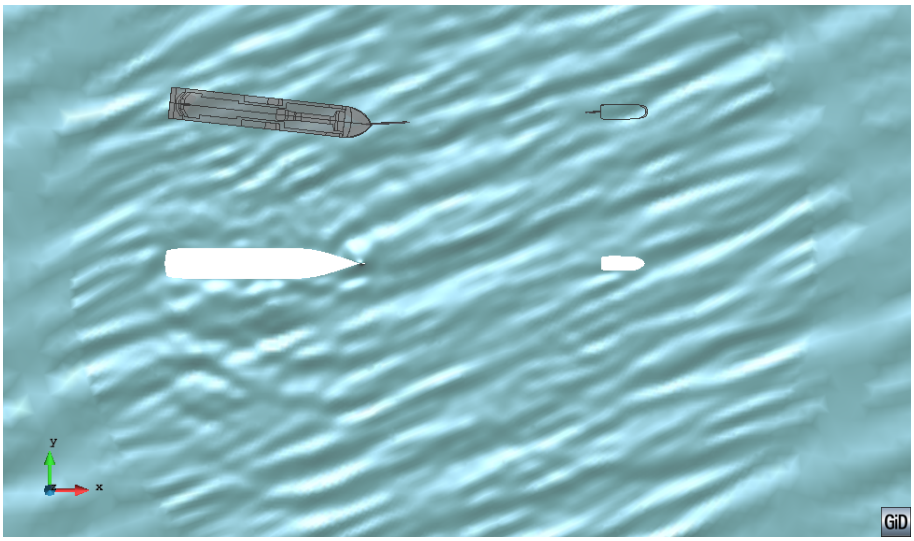

Figure 27: : Zenital view, t=300 s

The next image show the total elevation of the free surface at a certain time step:

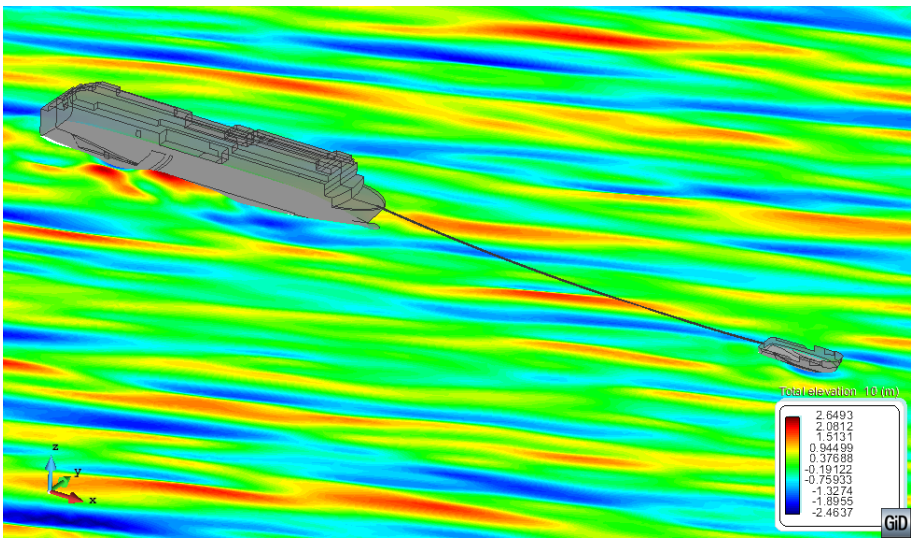

8. Conclusions

The main goal -and in this case also achievement- of this task, was to be able to create computer simulation case study model for assessing towing operation feasibility.

The simulations can provide, among other results:

- Time evolution of tension and displacements of the line.
- Quick, non-destructive testing procedure for towing lines.
- Damaged ship and tug boat dynamic response during the towing operations.
- Realistic visualization of the physical process, including towing line, tug boat and damaged ship responses, and free surface evolution.

Therefore, these simulations can eventually help to predict potential risks in rescue operations under different dangerous conditions: sea states, wind, or damage conditions (heeling, trim and sink) of the recovered ship.

In this deliverable, the results of a case study simulation have been presented, in order to show that previous statements have been fulfilled. Several iterations have been necessary to get to these results, mostly due to the lack of experience on actual towing operations. Fortunately, great support has been held from SASEMAR. This support has even included a technical guided visit to a tug boat sited in Barcelona port, in order to retrieve first-hand information.

Advice from the qualified personnel from SASEMAR has helped for example in taking in consideration the relevance of including drift effects, and also in a more accurate configuration of the different materials of the towing line.

Nevertheless, this report shows a case study, which will have to be followed by other future simulations, with different improvements, so as to being able to study different aspects as, for example:

- Including different towing line/s configurations.
- Stablishing standard, quick and non-destructive testing procedures for towing lines, using these CAE simulations.
- Creating quick response CAE models in order to simulate different situations in given scenarios, to assess actual rescue operations.

As a conclusion, it is not too risky to say that these simulation models can be a great starting point for future collaborations for achieving safety improvements regarding ship rescue operations. As has been done in this case, the aid of tug boat Captains and other experts can and will help CAE simulations to be optimized so as to properly reflect the actual rescue operation. This will improve the safety of the operation itself by providing quick results of the dynamic behaviour of the involved ships, together with the time evolution of the stresses on the tow lines.

Consequently, a dynamic feedback between software developers and marine experts can be achieved, boosting the efficiency of the simulations, or even providing new operational ideas. With adecuate training, the use of the software will allow to prepare and perform simulations of a certain emergengy situation, in a relatively short time.

Finally, we consider that simulations can also become a very efficient method for performing non-destructive tests for the ropes and cables of the towing lines, and therefore, foresee future problems and avoid accidents.

9. Annex I: Seakeeping/Manoeuvring code for simulations: SeaFEM

For performing the seakeeping, maneuvering/recovering simulations, the code chosen is **SeaFEM** (http://www.compassis.com/compass/SeaFEM), co-developed by CIMNE (http://www.cimne.com) and Compass IS (http://www.compassis.com).

SeaFEM is a suite of tools for the computational analysis of the effect of waves, wind and currents on naval and offshore structures, as well as for manoeuvring studies. **SeaFEM** has been developed for the most realistic seakeeping simulations of 3D multi-body radiation and diffraction problems, by solving **potential flow equations** in the **time domain**, using the **finite element method** (FEM) on **unstructured meshes**. The problem is formulated as follows:

$$\nabla^2\phi = 0, \quad \text{in } \Omega_f,$$

$$\partial_t\phi + u\nabla_h\phi + \frac{\nabla\phi_h^2}{2} + g\xi + \frac{P_a}{\rho} = 0, \quad \text{in } z = 0,$$

$$\partial_t\xi + (u\nabla_h\phi)\nabla_h\xi + \partial_z\phi = 0, \quad \text{in } z = 0,$$

$$\partial_z\phi = 0 \quad \text{in } z = -h,$$

$$(u + \nabla\phi)n_b = v_b n_b, \quad \text{in } z = \Gamma_b,$$

SeaFEM has been conceived to simulate seakeeping capabilities of ships and offshore structures, as well as calculating the hydrodynamic loads due to waves, currents, and translational velocities acting simultaneously. Moreover, the software has been equipped with the capability of introducing any external load acting over the structure under study. These external loads can be used to model aerodynamic loads, **mooring lines**, viscous effects such as damping and viscous resistance, **drift and/or wind forces**, or any other effect that might depend on any variable used by the program.

10. Annex: Cable model in SeaFEM for towing simulations

A new cable model which has been recently implemented in SeaFEM will be used for modeling the hawsers and ropes with tugboats used in towing operations.

10.1. Introduction

A brief introduction to the cable model used is explained in the following lines.

The cable model is based on the **dynamic analysis** of mooring systems. This analysis allows considering various effects over the cables, like flexion, torsion, elongation, inertia, vortex induced vibration or hydrodynamic effects. In this case, non linear **Finite Element Method** based in updated Lagrangian formulation has been used for determining the kinematic, dynamic and tension properties of the line, at each time step of the simulation. The tensions are the input to the global system, allowing to couple de mooring lines (ropes or hawsers) with the hydro-elastic behavior of the floating device analyzed, in this case, the damaged passenger ship.

In this model, the dynamics of the cable are estimated with straight bars connected by hinges, using the non linear FEM. The main hypotheses assumed are:

- Elastic material, with a defined elongation.
- Large length cables, with prevalence of axial rigidity.
- Cable´s tension changes along de longitudinal coordinate.

Some other effects are taken into consideration in the model, such as axial rigidity of the line, damping of the line, added mass effects, hydrostatic restoration and viscous drag forces generated by the fluid at each moment.

10.2. Formulation

It is possible to express the equations which rule de dynamics of the cable in matrix form. Therefore, given an external action $F(t)$, a position $x(t)$ can be found, which will verify the following equation:

$$\big(\mathbf{M} + \mathbf{MA}(t)\big)\ddot{x}(t) + \mathbf{C}\dot{x}(t) + \mathbf{K}x(t) = F(t)$$

Where **M** is the cable mass matrix, **MA** is the added mass matrix of each of the bars in which the cable is divided, **C** is the damping matrix of the cable, **K** is stiffness matix of the system and $F(t)$ is the nodal external forces acting on the cable line.
The mass of the line can be formulated using a consitent mass matrix, defined as:

$$\mathbf{M} = \mathbb{E}_i^n \, m^e$$

Where n is the number of line elements, $\mathbb{E}_i^n$ is a convenient assambler operator and m^e is the mass matrix of each cable segment, expressed as:

$$m^e = \int_0^{le} \mathrm{N}^T \rho \mathrm{N} \mathrm{d}s = \frac{A l_e \rho}{6} \begin{bmatrix} 2 & 0 & 0 & 1 & 0 & 0 \\ 0 & 2 & 0 & 0 & 1 & 0 \\ 0 & 0 & 2 & 0 & 0 & 1 \\ 1 & 0 & 0 & 2 & 0 & 0 \\ 0 & 1 & 0 & 0 & 2 & 0 \\ 0 & 0 & 1 & 0 & 0 & 2 \end{bmatrix}$$

Being N the the given position functions matrix, expressed as:

$$\mathrm{N} = \begin{bmatrix} \left(1 - \frac{x}{l^e}\right) & 0 & 0 & \frac{x}{l^e} & 0 & 0 \\ 0 & \left(1 - \frac{x}{l^e}\right) & 0 & 0 & l^e & 0 \\ 0 & 0 & \left(1 - \frac{x}{l^e}\right) & 0 & 0 & l^e \end{bmatrix}$$

The added masses may be formulated as:

$$\mathbf{MA} = \mathbb{E}_i^n \, ma^e$$

Where ma^e is the added mass of each slender bar:

$$ma^e = \rho A C_m \int_0^{le} \mathrm{N}^T \mathrm{N} \, \mathrm{d}s$$

Where C_m is the added mass coefficient.
The stiffness matrix is formulated taking into account the non-linearity of the problem, therefore, it is necessary to consider the tangential matrix:

$$\mathbf{K} = \mathbb{E}_i^n \, k^e$$

This tangential stiffness matrix can be obtained performing a total energy balance, and considering the stiffness as an internal energy (E_{int}) derived term with respect to the nodal displacements. The stiffness matrix of each element can be formulated as:

$$k^e = \frac{\partial \mathrm{E}_{int}}{\partial x} = \frac{\partial}{\partial x}\left(V^e f \frac{\partial e}{\partial x}\right) = V^e E \, \frac{\partial e}{\partial x} \otimes \frac{\partial e}{\partial x} + V^e f \frac{\partial^2 e}{\partial x^2} = k_o^e + k_l^e$$

Where the first term k_o^e represents the usual stiffness matrix for small displacements (Zienkiewicz and Taylor, 2005), while the second term k_l^e representas the large displacements of the bar elements. *E* represents the axial Young modulus, V^e represents the volume of the bar element, *e* is the unitary lengthement of the bar, and *f* is the stress on the bar per unit lenght, which can be expressed as:

$$\sigma = \sigma^o + Ee$$

being σ^o the initial or equilibrium state stresses of the cable.

The obtention of these matrixes can be read in bibliography relted with the FEM analysis in structures (Bathe, 1996; Hughes, 2000; Zienkiewicz and Taylor, 2005; Felippa, 2013) being k_o^e

$$k_o^e = V^e E \frac{\partial e}{\partial x} \otimes \frac{\partial e}{\partial x} = \int_0^{le} \mathrm{B}_o^T V^e E \mathrm{B}_o \mathrm{d}s = \frac{EA}{l_e} \begin{bmatrix} 1 & 0 & 0 & -1 & 0 & 0 \\ 0 & 0 & 0 & 0 & 0 & 0 \\ 0 & 0 & 0 & 0 & 0 & 0 \\ -1 & 0 & 0 & 1 & 0 & 0 \\ 0 & 0 & 0 & 0 & 0 & 0 \\ 0 & 0 & 0 & 0 & 0 & 0 \end{bmatrix}$$

being B_o^T the linear stress-displacement matrix, and $V^e E$ the material plasticity matrix.

$$k_l^e = V^e f \frac{\partial^2 e}{\partial x^2} = \int_0^{le} \mathrm{B}_l^T S \mathrm{B}_l \, \mathrm{d}s = \frac{\sigma}{l_e} \begin{bmatrix} 1 & 0 & 0 & -1 & 0 & 0 \\ 0 & 1 & 0 & 0 & -1 & 0 \\ 0 & 0 & 1 & 0 & 0 & -1 \\ -1 & 0 & 0 & 1 & 0 & 0 \\ 0 & -1 & 0 & 0 & 1 & 0 \\ 0 & 0 & -1 & 0 & 0 & 1 \end{bmatrix}$$

Being B_l^T the non-linear stress-displacement matrix and S the Piola–Kirchhoff stress tensor (Bathe, 1996).

En el modelo aquí descrito se ha empleado un amortiguamiento proporcional o de Rayleigh (Bathe, 1996), cuya expresión viene dada por,

$$\mathbf{C} = a_1 \mathbf{K} + a_2 \mathbf{M}$$

a_1 and a_2 are the mass and stiffness damping coefficients.

10.3. Forces acting on the line

The interaction of the cable with the surroindong fluid is expressed in a forces ballance:

$$F^e = \int_0^{le} \mathrm{N}^{\mathrm{T}} f^e \mathrm{N} \, \mathrm{d}s = F_w^e + F_h^e + F_d^e + F_f^e + F_o^e,$$

F_w^e is the gravity acceleration force, F_h^e is the vertical hydrostatic lift, F_d^e is the drag force due to currents, F_f^e is the force due to the eventual interaction with the oceaninc sea-bed and F_o^e is the drag force due to waves.

10.4. Temporay integration scheme

In this method, the dynamic of the line is solved in terms of acceleration, imposing boundary conditions in the line end points, which allow to make the cable movement compatible with the hydrodynamic analysis module *SeaFEM* (B. Serván and J. García–Espinosa, 2011;CompassIS,2014a).

In the dynamic case, the force ballance remains as follows:

$$(F^e)^{t+\Delta t} = \mathbf{M}^{t+\Delta t} \ddot{x} + \mathbf{C}^{t+\Delta t} \dot{x} + P^0 + (F_{int})^{t+\Delta t},$$

or,

$$(F^e)^{t+\Delta t} = \mathbf{M}^{t+\Delta t}\ddot{x} + \mathbf{C}^{t+dt}\dot{x} + P^0 + (F_{int})^{t+\Delta t} + \mathbf{K}^{t+\Delta t}\delta x,$$

$$\mathbf{M}^{t+\Delta t}\ddot{x} + \mathbf{C}^{t+\Delta t}\dot{x} + \mathbf{K}^{t+\Delta t}\delta x = (F^e)^{t+\Delta t} - P^0 - (F_{int})^{t+\Delta t}.$$

Therefore, the following dynamic ballance is obtained,

$$\mathbf{M}^{t+\Delta t}\ddot{x} + \mathbf{C}^{t+\Delta t}\dot{x} + \left(\mathbf{K}_{\mathbf{L}}^{t+dt} + \mathbf{K}_{\mathbf{G}}^{t+\Delta t}\right)\delta x = (F^e)^{t+\Delta t} - P^0 - (F_{int})^{t}.$$

Starting the iterative analysis, the line position is obtained, and the also a corresponding effective stress value. Therefore, the Newmark method may be written as

$$\left[\mathbf{M}^{t+\Delta t,i} + \gamma\Delta t\mathbf{C}^{t+\Delta t,i} + \beta\Delta t^2\left(\mathbf{K}_{\mathbf{L}}^{t+\Delta t,i} + \mathbf{K}_{\mathbf{G}}^{t+\Delta t,i}\right)\right]\ddot{x}^{t+\Delta t,i+1} =$$

$$= \beta\Delta t^2\left(\mathbf{K}_{\mathbf{L}}^{t+\Delta t,i} + \mathbf{K}_{\mathbf{G}}^{t+\Delta t,i}\right)\ddot{x}^{t+\Delta t,i} + (F^e)^{t+\Delta t} - P^0 - (F_{int})^{t+\Delta t,i}$$

$$-\mathbf{C}^{t+\Delta t,i}[\dot{x}^t + \Delta t(1-\gamma)\ddot{x}^t].$$

Resulting in a system:

$$\mathbf{M}_{\text{ef}}^{t+\Delta t,i}\,\ddot{x}^{t+\Delta t,i+1} = F_{\text{ef}}^{t+\Delta t,i},$$

where $\mathbf{M}_{\text{ef}}^{t+\Delta t,i}$ is the *'effective mass'* and $F_{\text{ef}}^{t+\Delta t,i}$ is the *'effective forces'* vector. Doing the same with the Bossak-Newmark scheme:

$$\left[(1-\alpha_b)\mathbf{M}^{t+\Delta t,i} + \gamma\Delta t\mathbf{C}^{t+\Delta t,i} + \beta\Delta t^2\left(\mathbf{K}_{\mathbf{L}}^{t+\Delta t,i} + \mathbf{K}_{\mathbf{G}}^{t+\Delta t,i}\right)\right]\ddot{x}^{t+\Delta t,i+1} =$$

$$= \beta\Delta t^2\left(\mathbf{K}_{\mathbf{L}}^{t+\Delta t,i} + \mathbf{K}_{\mathbf{G}}^{t+\Delta t,i}\right)\ddot{x}^{t+\Delta t,i} + (F^e)^{t+\Delta t} - P^0 - (F_{int})^{t+\Delta t}$$

$$-\mathbf{C}^{t+\Delta t,i}[\dot{x}^t + \Delta t(1-\gamma)\ddot{x}^t] - \alpha\mathbf{M}^{t+\Delta t,i}\ddot{x}^t.$$

The convergence is estimated in each time step and iteration, checking that the *Averge Cuadratic* Error remains below a certain given tolerance:

$$ACE = \frac{1}{n}\sum_{i=1}^{n}(x^{n+1} - x^n)^2.$$

10.5. Coupling with SeaFEM

Contrary to other works developed up to the date, in this development the seakeeping behavior of the floating device is obtained from the solution of the diffraction-radiation equations via the FEM, as for the cable dynamics, being this approach quite interesting given that the analysis is performed in the time domain, avoiding the use of techniques such as the convolution integral.

The link between the seakeeping and the cable analysis is presented schematically in the following steps:

1. Once SeaFEM has solved the velocities potential, the loop which solves the non linear dynamic of the floating device is started, for the current time step and the iteration *"i"* of the potential flow problem solver exterior loop.

2. With the velocities potential coming from SeaFEM, the pressure is determined in the fluid domain, and therefore, the forces and moments over the floater, integrating the pressures over it. That provides the dynamic behavior of the floater in the time step Δt.
3. The cable end position is then updated, imposing compatible accelerations with the estimated displacement. The new position of the cable end $\left(x_f, y_f, z_f\right)^{n+1}$, results:

$$x_f^{n+1} = x_f^n + \left(x_f + X^b + r_x\left(\cos\alpha^b \cos\beta^b - 1\right)\right.$$
$$+ r_y\left(\cos\alpha^b \ \text{sen}\beta^b \ \text{sen}\,\phi^b - \text{sen}\,\alpha^b \cos\phi^b\right)$$
$$\left. + r_z\left(\cos\alpha^b \ \text{sen}\,\beta^b \cos\phi^b + \text{sen}\,\alpha^b \,\text{sen}\,\phi^b\right)\right),$$
$$y_f^{n+1} = \left(y_f + Y^b + r_x\left(\cos\alpha^b \cos\beta^b\right)\right.$$
$$+ r_y\left(\text{sen}\,\alpha^b \ \text{sen}\beta^b \,\text{sen}\,\phi^b + \cos\alpha^b \cos\phi^b\right)$$
$$+ r_z\left(\text{sen}\,\alpha^b \ \text{sen}\,\beta^b \cos\phi^b - \cos\alpha^b \,\text{sen}\,\phi^b\right),$$
$$z_f^{n+1} = \left(z_f + Z^b + r_x\left(\text{sen}\,\beta^b\right) + r_y\left(\cos\beta^b \,\text{sen}\phi^b\right)\right.$$
$$\left. + r_z\left(\cos\alpha^b \cos\beta^b - 1\right)\right)$$

   Where $\left(r_x, r_y, r_z\right)$ are the floater rotations, and $\left(X^b, Y^b, Z^b\right)$ the loinear displacements.
4. For the first iteration *"j"* of the loop which solves de floater dynamics, the dynamic of the cable is calculated until convergence is reached, using the end´s displacement as a boundary condition. In the first iteration, the stiffness matrix of the cable is calculated, and will be used for linearizing the response of the cable en the current *"i"* iteration of the global solver.
5. The reactions (F_j) in the cable end are then used as exterior forces in SeaFEM, for calculating de floater dynamics, by means of the equation:

$$\bar{\bar{\boldsymbol{M}}}\left[(1-\alpha_b)\ddot{X}^{n+1} - \alpha_b \ddot{X}^n\right] + \bar{\bar{\boldsymbol{K}}} X^n = F^{n+1} + F_f$$

6. Iteration is performed until convergence in the dynamic loop is reached.
7. Once reached convergence, a new iteration of the exterior loop begins, until convergence in the global problem and then time step advances.

39 partners from 10 countries taking maritime transport into the digital age

By designing and demonstrating innovative use of ICT solutions MONALISA 2.0 will provide the route to improved

SAFETY - ENVIRONMENT - EFFICIENCY

Swedish Maritime Administration ◦ LFV - Air Navigation Services of Sweden ◦ SSPA ◦ Viktoria Swedish ICT ◦ Transas ◦ Carmenta ◦ Chalmers University of Technology ◦ World Maritime University ◦ The Swedish Meteorological and Hydrological Institute ◦ Danish Maritime Authority ◦ Danish Meteorological Institute ◦ GateHouse ◦ Navicon ◦ Novia University of Applied Sciences ◦ DLR ◦ Fraunhofer ◦ Jeppesen ◦ Rheinmetall ◦ Carnival Corp. ◦ Italian Ministry of Transport ◦ RINA Services ◦ D'Appolonia ◦ Port of Livorno ◦ IB SRL ◦ Martec SPA ◦ Ergoproject ◦ University of Genua ◦ VEMARS ◦ SASEMAR ◦ Ferri Industries ◦ Valencia Port Authority ◦ Valencia Port Foundation ◦ CIMNE ◦ Corporacion Maritima ◦ Technical University of Madrid ◦ University of Catalonia ◦ Technical University of Athens ◦ MARSEC-XL ◦ Norwegian Coastal Administration

www.monalisaproject.eu

Co-financed by the European Union
Trans-European Transport Network (TEN-T)